Radiotherapy and Oncology 107 (2013) 234–241

Contents lists available at SciVerse ScienceDirect

Radiotherapy and Oncology

journal homepage: www.thegreenjournal.com

Neutron contamination

Neutron contamination in radiotherapy: Estimation of second cancers based on measurements in 1377 patients

Maite R. Expósito [a,*], Beatriz Sánchez-Nieto [b], José A. Terrón [c], Carles Domingo [d], Faustino Gómez [e], Francisco Sánchez-Doblado [a,c]

[a] Departamento de Fisiología Médica y Biofísica, Universidad de Sevilla, Spain; [b] Departamento de Física, Pontificia Universidad Católica de Chile, Santiago, Chile; [c] Servicio de Radiofísica, Hospital Universitario Virgen Macarena, Sevilla; [d] Departamento de Física, Universitat Autònoma de Barcelona, Bellaterra; and [e] Departamento de Física de Partículas, Universidad de Santiago de Compostela, Spain

ARTICLE INFO

Article history:
Received 23 September 2012
Received in revised form 27 February 2013
Accepted 9 March 2013
Available online 16 April 2013

Keywords:
Peripheral dose
Neutron
Second cancer risk

ABSTRACT

Purpose: Second cancer, as a consequence of a curative intent radiotherapy (RT), represents a growing concern nowadays. The unwanted neutron exposure is an important contributor to this risk in patients irradiated with high energy photon beams. The design and development by our group of a neutron digital detector, together with the methodology to estimate, from the detector readings, the neutron equivalent dose in organs, made possible the unprecedented clinical implementation of an online and systematic neutron dosimetry system. The aim of this study was to systematically estimate neutron equivalent dose in organs of a large patient group treated in different installations.

Patients and methods: Neutron dosimetry was carried out in 1377 adult patients at more than 30 different institutions using the new neutron digital detector located inside the RT room. Second cancer risk estimates were performed applying ICRP risk coefficients.

Results: Averaged equivalent dose in organs ranges between 0.5 mSv and 129 mSv depending on the type of treatment (dose and beam-on time), the distance to isocenter and the linac model. The mean value of the second cancer risk for our patient group is 1.2%. Reference values are proposed for an overall estimation of the risks in 15 linac models (from 2.8×10^{-5} to 62.7×10^{-5} %/MU).

Conclusions: The therapeutic benefit of RT must outweigh the second cancer risk. Thus, these results should be taken into account when taking clinical decisions regarding treatment strategy choice during RT planning.

In the last few years, there has been a growing concern about second cancer induction associated with radiation treatments [1–6]. In its latest recommendations, the International Commission on Radiological Protection (ICRP) explicitly considers patient radiological protection [7].

Rapidly evolving radiation treatment technologies such as Intensity Modulated Arc Therapy or Intensity Modulated Radiation Therapy (IMRT) are able to produce a precise shaping of dose distributions, with a conformal avoidance of normal structures, which allows tumor dose escalation. The latter, together with the larger beam-on time associated with the inverse planning approach, implies an increased number of monitor units (MU) compared to the standard Conformal Therapy (CRT) [1,2], therefore leading to higher contributions of photon and neutron (energies above 10 MV) peripheral dose. Consequently, the task of including the risk of radiation-induced second cancers in the choice and optimization of treatment modality has an enormous importance [5]. This work focuses on the neutron contribution to peripheral dose, which is probably the most complex and least studied.

According to ICRP Publication 103 [7], the equivalent dose in a tissue or organ is the appropriate quantity to estimate the second cancer risk of the patient. Some recent works estimate this quantity for specific treatments [8–11] but, to our knowledge, no method has been developed to systematically provide the neutron equivalent dose in organs and the associated radiation-induced second cancer risk for any patient under radiotherapy (RT) treatment. A thorough description of a novel system developed by our group, based on a neutron digital detector placed in the treatment room [12] that allows the estimation of neutron equivalent doses in multiple organs of radiotherapy patients, can be found in Sánchez-Doblado et al. [13].

The aim of the present work was to apply that methodology to the estimation of neutron equivalent doses in organs in a large cohort of adult patients treated in a variety of conditions. A total of 1377 patients have been measured since 2008 in 31 different institutions. Additionally, and using existing risk models, a translation of the equivalent doses has been done in terms of the associated risk of developing a second cancer.

* Corresponding author. Address: Departamento de Fisiología Médica y Biofísica, Avda. Sánchez-Pizjuán, 41009 Sevilla, Spain.
E-mail address: mtromero@us.es (M.R. Expósito).

0167-8140/$ - see front matter © 2013 Elsevier Ireland Ltd. All rights reserved.
http://dx.doi.org/10.1016/j.radonc.2013.03.011

Patients and methods

Neutron detector

Measurements were performed with an active detector developed by our group. A thorough description of the detector was given by Gómez et al. [12]. This system is composed by an array of static random access memory chips mainly sensitive to thermal neutrons. Neutron interaction produces single-event upsets in memory chips and, after the irradiation, the amount of these upsets is computed. A piece of software, specifically designed, controls the reading process and also converts the events into neutron equivalent doses according to our model (see next subsection).

Neutron equivalent dose model

The methodology used for estimating the neutron equivalent dose in an organ is described in Sánchez-Doblado et al. [13]. Our model involved the convolution, at 16 reference points in an anthropomorphic phantom, of the normalized Monte Carlo[1] neutron fluence energy spectra with the kerma and the energy-dependent radiation weighting factor. These results were scaled by the total neutron fluence measured, at the same points, with passive detectors. Correlation models between the latter and the readings of the digital detector were developed for specific irradiation sites, field parameters and installations, which allowed the on-line estimation of neutron equivalent doses.

Neutron equivalent dose in organs

The detector was placed in front of the rotation gantry axis and close to the wall. This location prevents the device from receiving the direct incidence of the photon beam and avoids gantry angle dependence [14]. This position does not cause any inconvenience to patient or staff.

In summary, the neutron dose is calculated as follows:

$$H_T^{k,j} = DD^* \cdot g_{k,j}^n \quad (1)$$

where $H_T^{k,j}$ is the neutron equivalent dose (H_T) in the organ k of a patient subject to treatment j, DD^* is the detector reading during irradiation, corrected by specific calibration factors and bunker geometry, and $g_{k,j}^n$ are organ- and treatment-dependent correlation coefficients estimated in [13]. The organs which are relevant for radioprotection (thyroid, esophagus, lung, breast, stomach, liver, colon, urinary bladder, ovary, skin, bone, bone marrow and the remainder) have been selected for reporting the dose. The $g_{k,j}^n$ values were estimated with an uncertainty of ±30% (1SD).

There are other factors affecting the uncertainty in neutron equivalent dose in organs which will be discussed later. Therefore, the neutron equivalent dose in organs obtained using this methodology has, at least, an uncertainty of 30% (1SD). This is acceptable for personal dosimetry as indicated in the current recommendations for monitoring individuals [15].

Second cancer risk model

For second cancer estimates, we have followed ICRP-103 [7]. The risk estimates of this report are derived from incidence data, for specific tumor sites, when adequate dose response data are available (mainly from the Japanese Life Span Study [LSS], where exposure conditions corresponded to acute or high doses [>200 mSv]). However, ICRP-103 guidelines are intended to be followed in case of low-dose, continuous, or fractionated exposures. ICRP-103 uses a judged dose and dose-rate effectiveness factor (DDREF = 2) that generalizes the usually lower biological effectiveness of low doses and low dose rates radiation exposures. A different case is the high LET radiation (such as neutrons), for which some authors [16] do not apply such a correction, which is equivalent to multiplying by 2 the risk coefficients of the ICRP-103.

Thus, the nominal risk estimates for each organ k were calculated as follows:

$$R^{k,j} = 2 \cdot \lambda_k \cdot H_T^{k,j} \quad (2)$$

being λ_k the nominal risk coefficients (cases per 10,000 persons per Sievert) (table A.4.1 of ICRP-103). Coefficients for the whole population were selected instead of those for the working age population, given that the latter is restricted to the 18–64 year-old interval, and patients can be both older (frequently) and younger. Sex-specific data were not considered, as ICRP-103 recommends for the general purposes of radiological protection [7]. ICRP recommends the use of a Linear-non-threshold model for the low dose range. Dasu et al. [17], after comparing different risk models, also mentioned that a linear model could be a useful simplification for the low dose range.

The total risks TR_j associated with a specific irradiation were therefore estimated as follows:

$$TR_j = n \cdot \sum_k R^{k,j} \quad (3)$$

where the summation extends over all organs above listed and n is the total number of fractions of the radiotherapy treatment for which a single fraction was measured with the detector.

In case of a treatment having 2 or more series with different MUs (e.g., a first series for PTV and another one for boost), an effective number of sessions (n') was used, obtained from the following equation:

$$n' = \frac{MU_T}{MU_{med}} \quad (4)$$

being MU_T the number of MU of the complete treatment, and MU_{med} the MU of the measured session. This is a good approximation, given that TR mainly depends on MU (see results) whereas field size and beam entry angles' dependences are almost negligible [13].

All these operations have been programed in the control software of the digital detector.

Patients

Measurements with our digital detector were carried out during at least one session of a RT treatment on 1377 patients in 15 linac models (different combinations of linac manufacturer and nominal energy – ranging from 10 MV to 25 MV) in a total of 50 facilities. Measurements were performed for a large variety of tumor sites and techniques. However, for the sake of simplicity when presenting the results, pathologies were grouped into the following categories: breast, lung, prostate, pelvic region and head and neck. The pelvic category includes pathologies such as those of the rectum, the urinary bladder, and the gynecological region [18]. Prostate treatments were considered as a separate category given their particular relevance. In order to use our model for neutron dose estimation, breast, lung, prostate, and pelvic categories were considered as abdomen treatment types [13]. Table 1 describes the patient distribution among treatment categories and linac models.

[1] Our Monte Carlo simulation showed that normalized neutron spectra exhibit an almost equal distribution at the isocenter, regardless of linac manufacturer and energy. This universality of the primary spectral distribution is consequently extended to the moderated (i.e., in-phantom) neutron spectra.

Table 1
Distribution of patients undergoing the different treatments and for each linac.

	No. facilities	Head			Lung			Breast			Prostate			Pelvic region								Other	Total
														Urinary bladder			Rectum			Gynecologic			
		N	% New[a]	% Comb.[b]	*N*	% New	% Comb.	*N*	% New	% Comb.	*N*	% New	% Comb.	*N*	% New	% Comb.	N	% New	% Comb.	*N*	% New	% Comb.		
Elekta Axesse 10 MV	2										7	100											7	7
Elekta SL 15 MV	2	7		14	5		60	2		100	17						6			3			3	43
Elekta Precise 15 MV	2	2		50	2		50	8		100	9						2		50	2			6	31
Elekta Synergy 15 MV	1	2		100							12									1				15
Elekta Axesse 15 MV	1	3	67								3	67											4	10
Siemens Primus 15 MV	5	34	18	74	26		50	98		95	38	8	3	2			28		11	23	4	4	39	288
Siemens Oncor 15 MV	7	5	100	80	8	13	75	20	10	90	56	7		1			19	21	16	7			26	142
Varian Clinac 15 MV	7	15	13	87	16		31	25	4	88	47	46		6	17		17		24	17	29	6	44	187
Elekta SL 18 MV	1	1		100							10		100	1		100	3		100	2		100	5	22
Elekta Axesse 18 MV	1										6	67					2						2	10
Siemens Primus 18 MV	5	21	14	76	10	10	50	35	46	100	101	39	0	1	100	100	32	72	66	15	60	20	19	234
Siemens Oncor 18 MV	1	4		75	2			1		100	10		10	1			1			1			2	21
Varian Clinac 18 MV	12	30		73	18		11	35		94	107	1		11			43		21	14		14	69	327
Siemens Mevatron 23 MV	2				1			6		17	3									7		14	19	36
Saturne 25 MV	1				1		100																3	4
Total	50	124			89			230			426			23			152			92			241	1377

[a] Percentage of new techniques such as Intensity Modulated Radiation Therapy (IMRT), or Volumetric Modulated Arc Therapy (VMAT).
[b] Percentage of combined treatments, i.e., 6-MV beams together with high energy beams.

Results

For each patient, neutron equivalent doses in the selected organs were estimated. This whole data set was analyzed grouping the data by treatment category. Fig. 1 shows, as an example, the average neutron equivalent doses in organs of prostate cancer patients, for the 15 different linac models. Similar plots were obtained for the other treatment categories.

Our results show that, in organs closer to the central axis, the neutron equivalent dose is higher. For example, we assume that the liver in our model [13] is located at approximately 10 cm and 60 cm from the central axis for abdomen and head and neck treatments, respectively. Average neutron equivalent doses in liver were 5.29 μSv/MU and 1.94 μSv/MU during prostate and head treatments in an 18 MV Varian Clinac, respectively. That is, a factor of 2.7. On the basis of the paper by Kry et al. [19], this factor can be estimated at 1.3 for the same linac. When the same exercise was repeated for the Elekta Synergy 15 MV, doses to the liver resulted in 0.15 μSv/MU and 0.44 μSv/MU (a factor of 2.9). Equivalent doses per MU have been considered instead of absolute dose values to eliminate the effect of higher prescription doses (and consistently of MU) for prostate, compared to head treatments. For both treatments, liver doses per MU escalate by a factor of 12 from Elekta to Varian machines.

Table 2 shows the mean value (together with the maximum and minimum) of the neutron equivalent doses in all organs for the 15 different linac models and the 5 treatment categories. Differences among equivalent doses in organs (see Fig. 1 for prostate treatments) explain the wide dose range reported. For the same linac model, differences between treatment categories are mainly due to differences in prescription dose, treatment technique (with different efficiency in the number of MUs) and proportion of high energy beams used.

By applying Eqs. (2) and (3), TR values were calculated for the whole patient cohort. Fig. 2 shows the total neutron risk averaged out for the patients irradiated in each of the 15 linac models, grouped into the 5 treatment categories under study. In general, prostate treatments lead to the highest TR values, being the worst case treatments carried out with the 23 MV Siemens Mevatron linac, for which approximately 7% of treated patients would develop a second cancer, according to our estimates. This value decreases to approximately 3% for the 15 MV and 18 MV Varian Clinac linac models. For most treatment categories and linac models, the estimations for TR are around 1–2%.

The insert in Fig. 2 shows TR averaged values for prostate cancer patients irradiated in 15 MV Siemens Primus linacs, for different treatment techniques (3DCRT as well as forward[2] and inverse IMRT). This plot focuses on the impact of the RT technique, for a fixed treatment site and linac model. It can be observed that, in the case of the most demanding MU technique (inverse IMRT), the TR can increase up to 4 times, when compared to 3DCRT. Forward IMRT represents an intermediate case. Effectively, the average number of MU for the inverse IMRT treatment plotted in the insert is 31,554 vs. 9333 for the 3DCRT (factor of 3.4). This is mainly due to the "less efficient" use of the beam-on time for inverse planning IMRT, but also due to the dose escalation usually associated with IMRT protocols.

The neutron dose dependence on MUs was explicitly analyzed. The results showed that the equivalent dose in organs increased linearly with MUs of high energy beams (i.e., above 10 MV), with different slopes for the various linac models. Fig. 3 depicts this linear behavior for the neutron equivalent doses in the liver for pros-

[2] Forward IMRT can be used for step and shoot techniques allowing a better control on the number of beam segments and MU (i.e., providing a more efficient use of them).

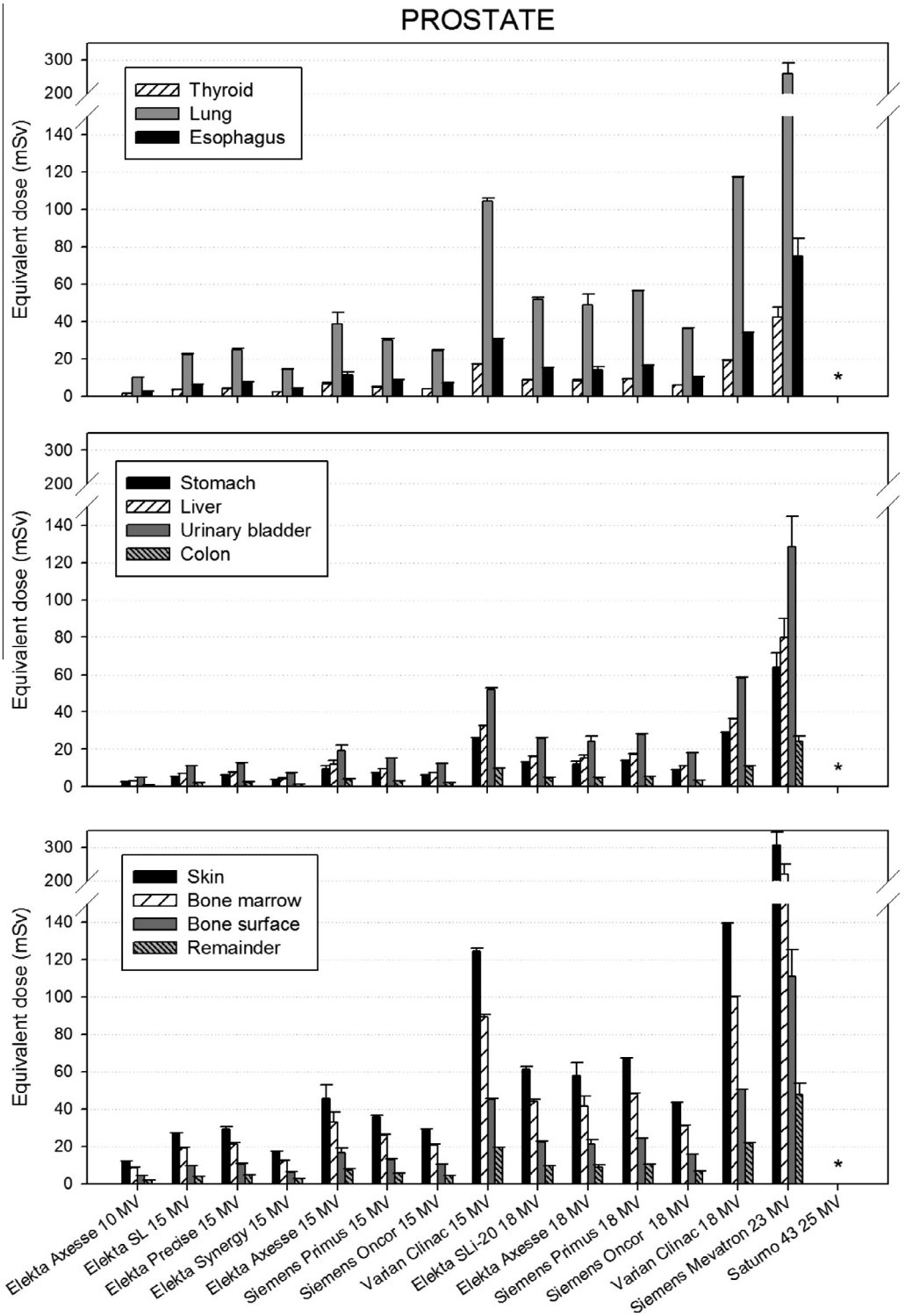

Fig. 1. Average neutron equivalent doses in each organ, for the different linac models, in prostate cancer treatments. Mean values and standard deviations (error bars) are displayed. *No patients available for this linac model.

tate cancer patients irradiated with the same energy (18 MV) but with three different linac models.

Owing to the use of a linear model for risk estimates, TR maintains such linearity (see Eqs. (2) and (3)). However, patient measurements were made for a large variety of real treatments (different from the standard treatments used for model development) and in very different bunker geometries, and both factors generate dispersion in the TR value predicted (error bars in Fig. 1). Therefore, a linear regression analysis was carried out to measure the strength of the association between TR and MU. A regression line was drawn for each linac model. The regression coefficients of the regression lines obtained for each linac model are presented in Table 2. The high values of the correlation coefficients reflect the high strength of the association between TR and MU.

Table 2
Neutron equivalent dose in organs (mSv) (mean, maximum and minimum doses) as a result of patient irradiation for different treatment sites, for each linac model. Last column represents our estimation of the second cancer total risks due to out-of-field neutron irradiation for each linac model.

Linac	Neutron equivalent dose in organs (mSv)												Total risk (cases per 1000 per 1000 MU) [a]
	Head and neck			Breast			Lung			Prostate			Pelvic region			
	Mean	Max	Min	Mean	Max	Min	Mean	Max	Min	Mean	Max	Min	Mean	Max	Min	
Elekta Axesse 10 MV										5.0	12	0.94				0.28 [b]
Elekta SL 15 MV	4.3	17	0.30	3.3	8.5	0.61	12.1	31	0.39	11	27	2.1	13	32	1.5	1.07 (0.85)
Elekta Precise 15 MV	4.4	18	0.31	1.7	4.4	0.35	9.6	23	1.8	12	30	2.3	9.0	23	0.53	0.91 (0.93)
Elekta Synergy 15 MV	0.5	2.0	0.034							7.1	17	1.3	3.5	8.9	0.70	0.45 (0.86)
Elekta Axesse 15 MV	11	45	0.79							19	46	3.6				0.83 (0.998)
Siemens Primus 15 MV	4.1	19	0.075	5.0	13	1.0	8.5	22	0.20	15	36	2.8	11	27	0.91	0.95 (0.85)
Siemens Oncor 15 MV	2.1	8.3	0.15	3.9	9.8	0.54	9.2	23.7	0.13	12	29	2.3	8.6	22	0.77	0.73 (0.88)
Varian Clinac 15 MV	6.2	26	0.26	12.5	32	1.9	16	42	1.1	52	124	9.8	25	65	2.9	1.99 (0.98)
Elekta SL 18 MV	10	41	0.72							26	61	4.8	15	37	1.0	2.11 (0.99)
Elekta Axesse 18 MV										24	58	4.6	31	80	2.9	1.24 (0.98)
Siemens Primus 18 MV	2.4	11	0.039	2.7	7	0.55				28	67	5.3	12	30	1.6	1.53 (0.92)
Siemens Oncor 18 MV	3.3	14	0.094	4.0	10	0.79	6.1	16	0.64	18	43	3.4	13	34	0.95	1.11 (0.96)
Varian Clinac 18 MV	13	53	0.67	14	35	2.7	44	112	0.53	58	139	11	41	105	4.0	4.74 (0.78)
Siemens Mevatron 23 MV				18	46	3.6	37	88	7.0	129	307	24	35	89	7.0	4.85 (0.99)
Saturne 25 MV							16	39	3.0							6.27 (0.999)

[a] Values between brackets represent the regression coefficients (R^2).
[b] The value presented is derived from an average of the ratios between total risk and MU. The small neutron production at 10 MV leads to high fluctuations in measured values which do not allow a reliable lineal regression procedure.

Discussion

In [13], a comprehensive study on neutron equivalent doses in organs of a standard man was carried out. Dependences on linac manufacturer, treatment energy, field sizes, beam entry angles, treatment location and bunker size were analyzed. Taking into consideration these factors, it was estimated that neutron equivalent doses in organs of a Norma-like standard man could be calculated with an uncertainty of ±30%.

However, there are other sources of uncertainties that must be considered. As mentioned in Sánchez-Doblado et al. [13], the selection of the points in NORMA representing each organ was made using the organ sizes and positions from the revised version of the Cristy anthropomorphic phantom (available at http://ordose.ornl.gov/resources/phantom). First, we represented the location of the organ centroid (specified by Cristy) inside our NORMA patient and we selected the closest detector locations taking into account the organ volume. This implies that, at least, we considered somehow the expected differences among the different subvolumes of an organ. This approach, consisting in defining a whole volume through only a few selected points, has some limitations. However, we believe that the complexity of experimental neutron dose evaluation amply justifies it.

Other factors which have not been included in our model yet are patient height and girth [19]. Therefore, our model was intended to estimate the neutron equivalent dose in organs of a "standard man/women". Some research is being conducted in order to investigate these patient size dependences. Neutron spectra resulting from whole real treatments, at 16 points in anthropomorphic phantoms representing an adult and two children (aged 10 and 5), have already been computed with MC [20]. Additionally, thermal neutron fluences have been measured in the same anthropomorphic phantoms using TLDs [21]. Our results show that, except for some points which are away from the isocenter (i.e., abdomen for head treatment and head for abdomen treatments), the neutron spectra resulting from the whole treatment (i.e., multiple incidences) almost matched up. Regarding thermal fluences, higher values have been found for the smaller phantoms as a consequence of less neutron attenuation, a finding that agrees with the results on neutron percent depth-dose equivalent from Kry et al. [19]. In order not to underestimate the dose applied to children, specific $g_{k,j}^{n}$ values should be determined. When reporting neutron equivalent dose in an organ (for the patients included in the study, the average values), for a specific treatment category and linac model, another source of heterogeneity appears (error bars in Fig. 1). This is mainly due to the fact that patients were treated in different institutions with treatments mainly differing in prescription dose and technique. Also, differences in the treatment plan design from center to center, which can combine high and low energies, contribute to differences in doses. For example, a different ratio of high to low energies increases the mentioned heterogeneity and can also explain the somehow surprising results, such as finding lower neutron doses for 18 MV Siemens linacs than for 15 MV Siemens linacs (e.g., see head and neck values in Table 2 for the 15 MV and 18 MV Siemens Primus).

Making a comparison with the neutron doses measured or simulated in other works is not an easy task because of the differences among methodologies for dose estimation (with their own associated uncertainties) and also because, in general, the reported values refer to very specific conditions (linac, energy, treatment site, etc.), whereas our results are representative of a pool of linac models, treatment sites, and techniques. Fig. 4 depicts neutron equivalent doses in a set of common organs during prostate irradiation, reported in different studies [9–11]. Bearing in mind the complexity of neutron dosimetry, where high uncertainties are expected (and acceptable), results are, at least, congruent.

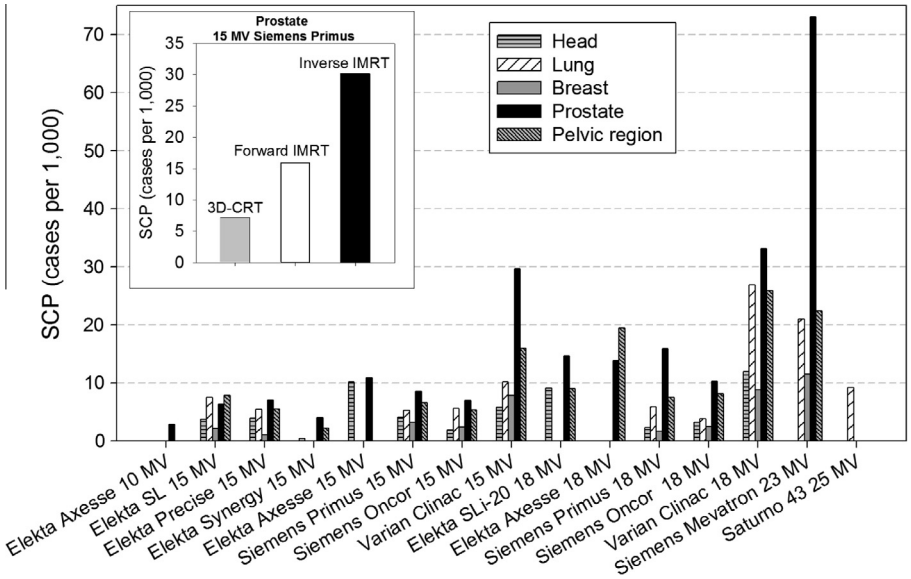

Fig. 2. Average of total risk values estimated for the patients grouped under each treatment category and treated with a specific linac model. The insert shows, for the 15 MV Siemens Primus linac model, the average total neutron risk split into 3 different prostate treatment strategies (3D-CRT and forward and inverse IMRT).

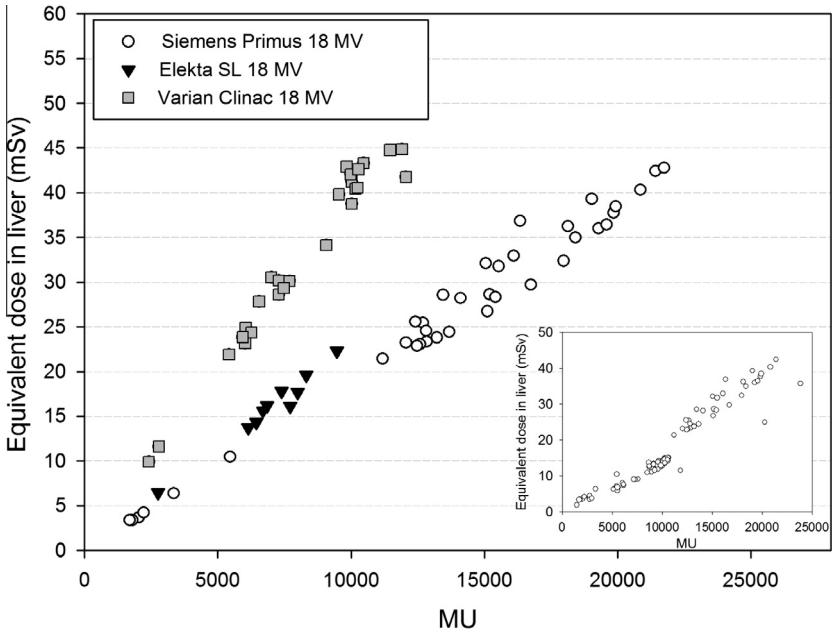

Fig. 3. Neutron equivalent doses in the liver versus MU, estimated for prostate cancer patients irradiated with 18 MV for three linac models (one for each manufacturer). For the sake of clarity, only patients from a single institution were chosen for each linac model. The higher dose increase per MU, for the Varian Clinac with respect to the other two specific models, is representative of what has been observed between the three manufacturers (see risk estimations for each model in Table 2). The insert represents neutron dose to liver for all 101 prostate cancer patients from this study irradiated with Siemens Primus machines operating at 18 MV. It can be seen that inter-institution differences do not affect the linear behavior.

The mean value of the TR for the 1377 patients is 1.2%, 1.6% if exclusively high energy patients are considered, and 0.6% for treatments combining high and 6 MV energy beams. Although those risks seem small in general, their relevance is large because of the great amount of patients treated every year. Vano [22] estimated a value of 5.1 million courses of RT treatment administered annually between 1997 and 2007. According to our most favorable risk estimation (0.6% incidence risk) and assuming that about a third was treated with high energy [23], 10,200 patients might develop a second cancer every year.

Our estimations correspond to second cancer risk due to neutrons, expressed as a function of the MU of high energy beams. In order to test whether or not our estimations provide reasonable figures, a comparison between our total second cancer risk, due exclusively to neutron irradiation, and the results from epidemiologic studies should be carried out. However, it is obvious that those studies cannot distinguish between the second cancers attributable to neutrons and the ones caused by photons. In Bartkowiak et al. [24], an incidence rate of ~4% (493 cases in a population of 12,000 patients) was estimated for second cancers due to peripheral doses. An attributable risk of 8% has been published by Berrington et al. [25] for their radiotherapy patients (i.e., $\geqslant$1 year survivors). The application of our methodology to 1377 patients, all of them treated with high energy beams, provided a mean value

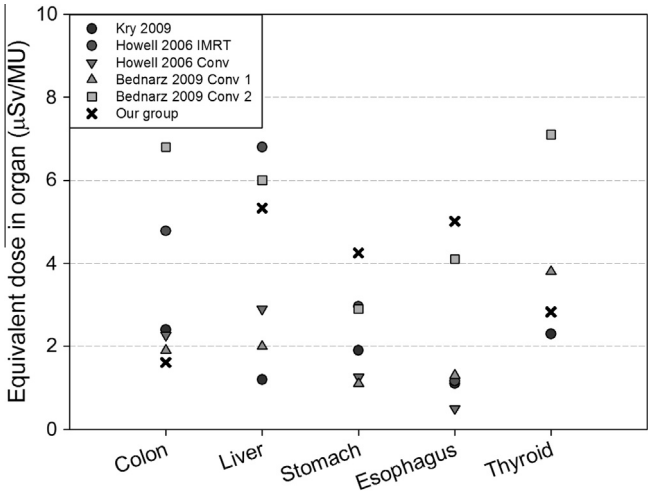

Fig. 4. Neutron equivalent dose per MU in a set of common organs for prostate treatments in an 18 MV Varian Clinac. Results from other works were obtained experimentally [10] and by MC simulation [9], [11].

of 1.2% for the total risk due to neutrons. The same value can be obtained from Table 2 for the average value of high energy MU of the 1377 patients. These figures are consistent, as our risks only take into account the neutron irradiation.

In order to analyze the reason for the highest risk value, observed for the prostate treatments with the Siemens Mevatron 23 MV, we compared it with the one obtained for the same type of treatment with the Varian Clinac 18 MV. A factor of 2.2 was found. This can be explained by the higher number of MU (14,695 for the Siemens Mevatron 23 MV vs. 6805 for the Varian Clinac 18 MV, exactly a factor of 2.2).

Additionally, it can be noticed that for the same treatment site and linac manufacturer, TR still shows variability as a consequence of the different treatment techniques used for those patients as shown in insert in Fig. 2. The average 1% TR estimated for prostate treatments carried out in the Siemens Primus 15 MV splits in 3 different values depending on the treatment technique (i.e., which affects the number of MU). Therefore, a note of caution should be put upon the statement that prostate treatments delivered with a certain machine have a certain level of associated risk, as TR will necessarily increase if the proportion of more demanding MU techniques increases.

Our comprehensive set of measurements allowed us to quantify the magnitude of that increase. In particular, a linear association was found, with different slopes depending on the linac model. For a fixed energy, the slope depends on the linac manufacturer (the higher the slope, the higher the impact of MU on the peripheral neutron dose is). It is worth emphasizing that this is true regardless of the number of beams, beam entry angles and field sizes, indicating that the neutron production is mainly dependent on the beam-on time and linac model (manufacturer and energy). It is therefore recommendable to estimate and record the total risk values as a function of the number of MUs for each linac model as reported in Table 2.

For a given nominal energy, risk depends strongly on linac manufacturer. Varian linacs lead to higher risk than Siemens linacs, in agreement with results from other works [26–28], while Siemens Oncor linacs produce smaller risk than previous models like Primus.

It is worth noticing that values reported in Table 2 can be used to estimate the overall TR value which should be expected for a patient population irradiated with the specific linac model, as a function of the MU used for treatment delivery, regardless of treatment site and technique. The latter is, nevertheless, a very good approximation as the regression coefficients were very high, reflecting that MU and linac model are, by far, the most important parameters determining the TR associated with neutron contamination. Only the Varian Clinac 18 MV regression model does not fit so well our set of data (R^2 = 0.78). A deeper insight into the data seemed to suggest that, from the point of view of neutron production, there are two "different" Varian Clinacs which do not follow any Varian classification for the Clinac 2100C family. Further research to clarify this issue is being conducted.

The methodology used for the results presented in this work is based on a comprehensive set of experiments and simulations which take into account all the possible parameters that could influence neutron production and neutron dose deposition in organs. In spite of the complexity of the problem, the procedure has proved to be simple and universal. During the process of measuring neutron doses for the 1377 patients, the system never caused any interference with the patient treatments or any trouble to staff. Therefore, it has been tested for clinical applicability with a complete success.

These experimental models are currently being tested on a different patient group by comparing the differences between the predictions and the actual TR estimation calculated after the measurements with the digital detector.

Conclusions

To our knowledge, this is the first time that, in a direct and systematic way based on a novel neutron digital detector designed by our group, an estimation of second cancer induction due to neutron contamination has been carried out on such a large group of patients undergoing radiotherapy.

The neutron equivalent dose in organs, estimated for 1377 patients, depends on distance from the organ to the irradiated volume, machine manufacturer, nominal photon energy and number of MUs (which basically depends on prescription dose and efficiency of the treatment technique to deliver the required dose). Maximum values above 200 mSv for the lung and skin have been estimated for prostate treatments in a machine operating at 23 MV, whereas only a few mSv were calculated for 10 MV or even 15 MV machines in other organs. The highest neutron dose, and consequently the total risk of developing a second cancer, corresponds to prostate treatments with irradiations of 15 and 18 MV.

Neutron equivalent dose in organs showed a linear dependency with the beam-on time which is reflected in the total risk estimations. The rate at which TR increases with MU mainly depends on the linac model. According to these results, and in order to allow an overall estimation of TR for any number of MU for the 15 linac models, reference TR values per 1000 MU have been proposed. The latter should be used as extra information for taking clinical decisions regarding treatment strategy choice during treatment planning.

Acknowledgements

The authors are indebted to the Andalusian Health Service (SAS) for its support through a University Law (LOU) contract with the University of Seville, to the Spanish Ministry of Science and Technology for its support through grant agreements PET2006_0412 and FIS2009-10634, and especially to the Spanish Nuclear Security Council for its support through a specific agreement with the University of Seville for measuring neutron doses in radiotherapy patients.

The experimental measurements would have been impossible without the kind collaboration of the radiophysicists and technicians in the different hospitals, in particular: R. Arráns, G. Sánchez,

M. Herrador, J.C. Mateos, J. Roselló, L. Brualla-González, S. Díaz, V. Crispín, J. Pérez-Calatayud; A. Sánchez-Reyes, M. Ribas and A. Latorre, C. Saez, E. Luguera, M.C. Lizuain, J. Vilar, L. Escudé, G. Hartmann, G. Sroka-Pérez, O. Schramm, A. Hernández, P. Ortega, P. Fernández-León, J. Torres, F. García, L. Martínez, J.D. Azcona, L. Ramos, J.M. Ordiales, R. Steurer, E. Nwabueze, M. Rodríguez-Ponce, M. Rodríguez-Villafuerte, Igor and Peter, A. Chervyakov, T. Bochkareva, M. Fomintseva, D. Grishchuk, E. Kuznetsova, T. Ponezha, E. Baranov, C. Sandín, S. Moral-Sánchez, L. Bragado-Álvarez, A. Guisasola-Berasategui, D. Planes, D. Esposito, M.C. Lopes, B. C. Ferreira, M. Melchor and D. Martínez.

We would also like to thank H. Galán-Dorado for her revision of grammar and style.

References

[1] Hall E-J, Wuu C-S. Radiation-induced second cancer: the impact of 3D-CRT and IMRT. J Radiat Oncol Biol Phys 2003;56:83–8.
[2] Hall E-J. Intensity-modulated radiation therapy, protons, and the risk of second cancers. J Radiat Oncol Biol Phys 2006;65:1–7.
[3] Hall E-J. Is there a place for quantitative risk assessment? J Radiol Prot 2009;29:A171–84.
[4] Milecki P, Adamska A, Roszak A, et al. Should be affraid of induced cancer in group of patients after radical radiotherapy of prostate cancer? Rep Pract Oncol Radiother 2009;14:184–90.
[5] Trott K-R. Can we reduce the incidence of second primary malignancies occurring after radiotherapy? Radiother Oncol 2009;91:1–3.
[6] Xu X-G, Bednarz B, Paganetti H. A review of dosimetry studies on external-beam radiation treatment with respect to second cancer induction. Phys Med Biol 2008;53:R193–241.
[7] International Commission on Radiological Protection. The 2007 recommendations of the International Commission on Radiological Protection. Elsevier, ICRP Publication 2007;103.
[8] Barquero R, Edwards TM, Íñiguez MP, et al. Monte Carlo simulation estimates of neutron doses to critical organs of a patient undergoing 18 MV X-ray LINAC-based radiotherapy. Med Phys 2005;32:3579–88.
[9] Bednarz B, Hancox C, Xu X-G. Calculated organ doses from selected prostate treatment plans using Monte Carlo simulations and an anatomically realistic computational phantom. Phys Med Biol 2009;54:5271–86.
[10] Howell RM, Hertel NE, Wang Z, et al. Calculation of effective dose from measurements of secondary neutron spectra and scattered photon dose from dynamic MLC IMRT for 6 MV, 15 MV, and 18 MV beam energies. Med Phys 2006;33:360–8.
[11] Kry SF, Salehpour M, Titt U, et al. Monte Carlo study shows no significant difference in second cancer risk between 6 and 18 MV intensity-modulated radiation therapy. Radiother Oncol 2009;91:132–7.
[12] Gómez F, Iglesias A, Sánchez-Doblado F. A new active method for the measurement of slow-neutron fluence in modern radiotherapy treatment rooms. Phys Med Biol 2010;55:1025–39.
[13] Sánchez-Doblado F, Domingo C, Gómez F, et al. Methodology and benchmark dataset for radiotherapy real time assessment of patient neutron dose with a novel digital detector. Phys Med Biol 2012;57:6167–91.
[14] Jiménez-Ortega E, Expósito MR, González-Soto X, et al. Characterization of the neutron induced single event upset in SRAM around high megavoltage clinical accelerators. In: 12th European conference on radiation and its effects on components and systems (RADECS) 2011. p. 922–5.
[15] European Commission. Technical recommendations for monitoring individuals occupationally exposed to external radiation. Radiat Protect 2009;160.
[16] Athar B, Paganetti H. Comparison of second cancer risk due to out-of-field doses from 6-MV IMRT and proton therapy based on 6 pediatric patient treatment plans. Radiother Oncol 2011;98:87–92.
[17] Dasu A, Toma-Dasu I, Olofsson J, et al. The use of risk estimation models for the induction of secondary cancers following radiotherapy. Acta Oncol 2005;44:339–47.
[18] Terrón JA, Expósito MR, Barquero R, et al. Neutron dose in pelvic radiotherapy treatment location. Radiother Oncol 2011;99:S557.
[19] Kry S-F, Howell R, Salehpour M M, Followill DS. Neutron spectra and dose equivalents calculated in tissue for high-energy radiation therapy. Med Phys 2009;36:1244.
[20] Gónzalez-Soto X, Expósito MR, Sánchez-Nieto B, et al. Neutron spectra inside an adult and children anthropomorphic phantoms in high energy radiotherapy. In: Long M, editor. WC 2012, IFMBE Proceedings 39. Berlin: Springer; 2012. p. 1145–8.
[21] Sansaloni F, Lagares JI, Muñiz JL, et al. Peripheral gamma dose and thermal neutron fluencies evaluation for IMRT on adult, teen and child. Radiother Oncol 2011;99:S558.
[22] Vano E. Global view on radiation protection in medicine. Radiat Prot Dosim 2011;147:3–7.
[23] Hall EJ, Martin SG, Amols H, et al. Photoneutrons from medical linear accelerators – radiobiological measurements and risk estimates. Int J Radiat Oncol Biol Phys 1995;33:225–30.
[24] Bartkowiak D, Humble N, Suhr P, et al. Second cancer after radiotherapy, 1981–2007. Radiother Oncol 2012;105:122–6.
[25] Berrington de Gonzalez A, Curtis RE, Kry SF, et al. Proportion of second cancers attributable to radiotherapy treatment in adults: a cohort study in the US SEER cancer registries. Lancet Oncol 2011;12:353–60.
[26] Howell RM, Kry SF, Burgett E, et al. Secondary neutron spectra from modern Varian, Siemens, and Elekta linacs with multileaf collimators. Med Phys 2009;36:4027–38.
[27] Kry SF, Salehpour M, Followill DS, et al. Out-of-field photon and neutron dose equivalents from step-and-shoot intensity-modulated radiation therapy. J Radiat Oncol Biol Phys 2005;62:1204–16.
[28] Martínez-Ovalle SA, Barquero R, Gómez-Ros JM, et al. Neutron dose equivalent and neutron spectra in tissue for clinical linacs operating at 15, 18 and 20 MV. Radiat Prot Dosim 2011;147:498–511.